

Corrosion prediction of metallic cultural heritage assets by EIS

*Original*

Corrosion prediction of metallic cultural heritage assets by EIS / Angelini, E.; Grassini, S.; Parvis, M.; Zucchi, Fabrizio. - In: CORROSION SCIENCE AND TECHNOLOGY. - ISSN 1598-6462. - STAMPA. - 18:4(2019), pp. 121-128. [10.14773/cst.2019.18.4.121]

*Availability:*

This version is available at: 11583/2752737 since: 2020-05-12T13:56:50Z

*Publisher:*

Corrosion Science Society of Korea

*Published*

DOI:10.14773/cst.2019.18.4.121

*Terms of use:*

This article is made available under terms and conditions as specified in the corresponding bibliographic description in the repository

*Publisher copyright*

(Article begins on next page)

# Corrosion Prediction of Metallic Cultural Heritage Assets by EIS

E. Angelini<sup>1,†</sup>, S. Grassini<sup>1</sup>, M. Parvis<sup>2</sup>, and F. Zucchi<sup>3</sup>

<sup>1</sup>*Dipartimento di Scienza Applicata e Tecnologia, Politecnico di Torino, Torino, Italy*

<sup>2</sup>*Dipartimento di Elettronica e Telecomunicazioni, Politecnico di Torino, Torino, Italy*

<sup>3</sup>*Dipartimento di Chimica, Università di Ferrara, Tecnehub, Ferrara, Italy*

(Received March 12, 2019; Revised August 23, 2019; Accepted August 23, 2019)

Electrochemical Impedance Spectroscopy (EIS) was used to predict corrosion behaviour of metallic Cultural Heritage assets in two monitoring campaigns: 1) an iron bar chain exposed indoor from over 500 years in the Notre Dame Cathedral in Amiens (France); and 2) a large weathering steel sculpture exposed outdoor from tens of years in Ferrara (Italy). The EIS portable instrument employed was battery operated. In situ EIS measurements on the iron chain could be used to investigate the phenomena involved in the electrochemical interfaces among various corrosion products and assess and predict their corrosion behaviour in different areas of the Cathedral. Meanwhile, the sculpture of weathering steel, like most outdoor artefacts, showed rust layers of different chemical composition and colour depending on the orientation of metal plates. The EIS monitoring campaign was carried out on different areas of the artefact surface, allowing assessment of their protective effectiveness. Results of EIS measurements evidenced how employing a simple test that could be performed in situ without damaging the artefacts surface is possible to quickly gain knowledge of the conservation state of an artefact and highlight potential danger conditions.

**Keywords:** *Electrochemical impedance spectroscopy (EIS), Cultural heritage, Weathering steels, Ancient iron, Atmospheric corrosion*

## 1. Introduction

Cultural Heritage assets help to provide and preserve social, cultural, and educational resources. The often irreplaceable buildings, monuments, and settlements contribute to tourism and economic development, resulting in job creation and income generation. Climate stressors can directly affect cultural heritage buildings, monuments, and settlements. Sea level rise threatens coastal assets with increased erosion and salt water intrusion [1,2]. More frequent and intense storms and flood events can damage structures that were not designed to withstand prolonged structural pressure, erosion, and immersion. Changing precipitation patterns can quickly erode assets built for a different climate. Increases in soil moisture due to increased precipitation can reduce the physical stability of historic buildings and archaeological remains. Warmer temperatures and increased humidity can damage building materials and structures by encouraging rot, pest infestations, and erosion. Drought, warmer temperatures, salt weathering, and erosion threaten cultural heritage assets in des-

ert areas, built with dry stone and mud brick. In order to avoid a total degradation, the Cultural heritage-related adaptation options include: increasing necessary skillsets among stakeholders; changing management practices and policies related to infrastructure maintenance, reinforcement, and development to protect and fortify structures; developing partnerships that include benefits sharing, since the people seeking to preserve a site may be different from those whose actions are required to protect it. Main streaming adaptation strategies into existing cultural heritage management plans and programs can strengthen long-term preservation efforts [3]. When Cultural Heritage assets are rehabilitated, renovated, and monitored, all relevant long-term factors should be taken into account. While some adaptation measures for Cultural Heritage assets are similar to those for other kinds of infrastructure, Cultural Heritage assets also present unique challenges, as a matter they are generally not replaceable. In addition, some adaptation strategies are specific to heritage assets, such as combining traditional materials and skills with modern engineering when reinforcing, stabilizing and renovating historic assets to both preserve their historic aesthetics and enhance their longevity [4-6]. For metallic Cultural

<sup>†</sup>Corresponding author: [emma.angelini@polito.it](mailto:emma.angelini@polito.it)

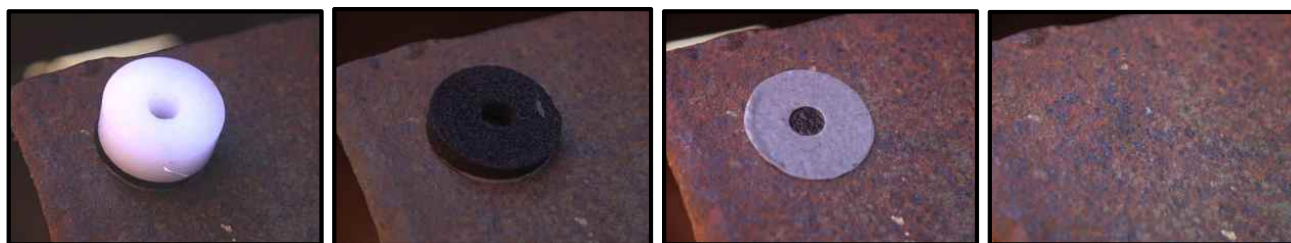


Fig. 1 The probe designed for the in situ EIS measurements. From left to right the removal of the probe after the EIS measurement, with no damage on the weathering steel surface.

Heritage assets the scientific approach to the conservation is mainly based on the concept of preventive conservation, based on the concept that deterioration is not inevitable and 'aging' is only the result of known and generally controllable causes, most of them, as mentioned above, are environmental, such as light, temperature, humidity, gaseous pollutants and aggressive chemical compounds [7,8]. Understanding the degradation mechanisms which affect the artefacts, as a function of the chemical composition, the production technique, the composition and stability of the corrosion product layers, is therefore, the starting point for developing tailored approaches for stopping degradation and preventing further damages [9-11].

Non-invasive techniques employed to assess the conservation state of metallic artefacts by means of in situ measurements are consequently very important tools for restorers and art historians to obtain valuable information on the artefact conservation state and the stability of the restoration treatment. Since corrosion is an electrochemical reaction, electrochemical techniques exhibit the unique possibility to provide direct access to the corrosion rate and do not need indirect measurement of the time dependence of the corrosion product formation [12-13]. The electrochemical techniques, because of their high sensitivity, cover the full range of corrosion rates from extremely stable to highly unstable materials.

Among the electrochemical techniques extensively employed for corrosion inspection and monitoring, such as linear polarisation resistance, electrochemical noise, acoustic emission, thin-layer activation, etc., electrochemical impedance spectroscopy (EIS) is probably the most important one employed to investigate the protective effectiveness of spontaneously grown surface layers, as bronze patinas, or coatings deliberately applied on metals and alloys [14-15]. EIS presents the advantage of applying a very small perturbation to the system, thus avoiding the acceleration of the corrosion process, and, can be repeated at increasing time periods to highlight the presence of dangerous situations and the need of restoration. Moreover,

EIS measurements may be performed in situ; this possibility is of outstanding importance with metallic Cultural heritage asset, because of the wide range of dimensions, that can make them immovable.

This paper reports the results of two monitoring campaigns carried out by means of in situ EIS measurements in order to acquire information on the conservation state of an indoor Cultural Heritage asset, an iron bar chain in the Notre-Dame Cathedral of Amiens (France) and an outdoor Cultural Heritage asset, a weathering steel sculpture in Ferrara (Italy).

## 2. Experimental Procedure

The EIS measurements were carried out by means of a portable equipment specifically designed by the authors to perform in situ monitoring [16,17]. Some commercially available EIS instruments are battery operated and employ an USB interface for both supplying the instrument and transferring the data to a PC, however, their design, which usually includes the possibility of performing cyclic voltammetry and other electrochemical tests, makes them quite expensive. On the contrary, the authors have developed low cost compact EIS systems, which provide all the required measurement facilities. The main features of the device are: i) recording of EIS spectra in a wide frequency range, 1 mHz to 100 kHz; ii) generation of both the AC sinusoidal stimulus and the DC bias voltage, necessary for the potentiostatic function; iii) synchronous sampling of voltage and current, measured by means of a transimpedance amplifier in order to compute the impedance; iiiii) impedance measurements in the range 1 k $\Omega$  - 10 G $\Omega$ . In all devices, the measurement accuracy, obtained by means of autocalibration techniques, is few percent in the impedance amplitude and few degrees in the phase.

The battery operated EIS instrument used in this paper may act as a stand-alone device, thus storing the results into its memory, or can be connected to a personal computer thus allowing to follow the evolution of the im-

pedance measurement in real time. It works in the frequency range 10 mHz - 40 kHz and can measure impedances in the range 1 k $\Omega$  - 10 G $\Omega$ . The measurement is performed by stimulating the sample with a small alternating voltage, 10 - 100 mV, while compensating the open corrosion potential ( $E_{OCP}$ ).

The probes, designed by the authors, employed in the in-situ measurements on the metallic artefacts are shown in Fig. 1. The probe is constituted by a small teflon cylinder (15 mm high, 30 mm in diameter) with a central hole, 8-10 mm in diameter, and a Pt electrode located on its wall. The probe is fixed to the sample by means of a commercially available adhesive tape, which can be easily removed after the measurement, without affecting the surface conditions. A soft foam disk, 3 mm thick, is inserted between the adhesive and the cylinder for optimum adaptation to the surface.

The EIS measurements were carried out after a 30 min preconditioning step of the electrodes surface with mineralized water, in order to avoid lose of information both on the diffusion process and on the ionic charge transfer processes. In order to assess the corrosion layer stability and the EIS measurement reproducibility, on every measuring area, three probes have been positioned. As other properties of materials that benefit from modelling, EIS too utilizes the equivalent circuit modelling [18]. The behaviour of each element of the cell is described in terms of classical electrical components, as resistors, capacitors, inductors, as well as tailored electrochemical elements, as Warburg diffusion elements.

### 3. Results and discussion

#### 3.1 Indoor cultural heritage asset

The first case study is a wrought iron bar chain of the Notre Dame Cathedral in Amiens, the tallest complete cathedral in France, built between 1220 and 1270 and listed



Fig. 2 Notre Dame Cathedral in Amiens.

as a UNESCO World Heritage Site since 1981, Fig. 2. The iron bar chain was installed around late Middle Ages around the triforium level to correct a structural defect. The original design of the flying buttresses around the choir of the Cathedral had them placed too high to counteract the force of the ceiling arch pushing outwards resulting in excessive lateral forces being placed on the vertical columns. The structure was secured by placing a second row of more robust flying buttresses that connected lower down on the outer wall. This fix failed to counteract similar issues with the lower wall, which began to develop large cracks: the wrought iron bar chain, shown in Fig. 3, was put to resist the forces pushing the stone columns outward. The iron bar chain is covered by corrosion products constituted by iron oxides and oxy-hydroxides organised in a very complex structure, determined by micro-Raman analysis [19]. The corrosion products are mainly composed by high percentages of ferridryte (46 - 57%) and goethite (28 - 35%), while the akaganeite (5 - 13%) and lepidocrocite (2 - 11%) fractions are quite small. Furthermore the morphological characterisation of



Fig. 3 Different areas of the iron bar chain with different degradation degrees.

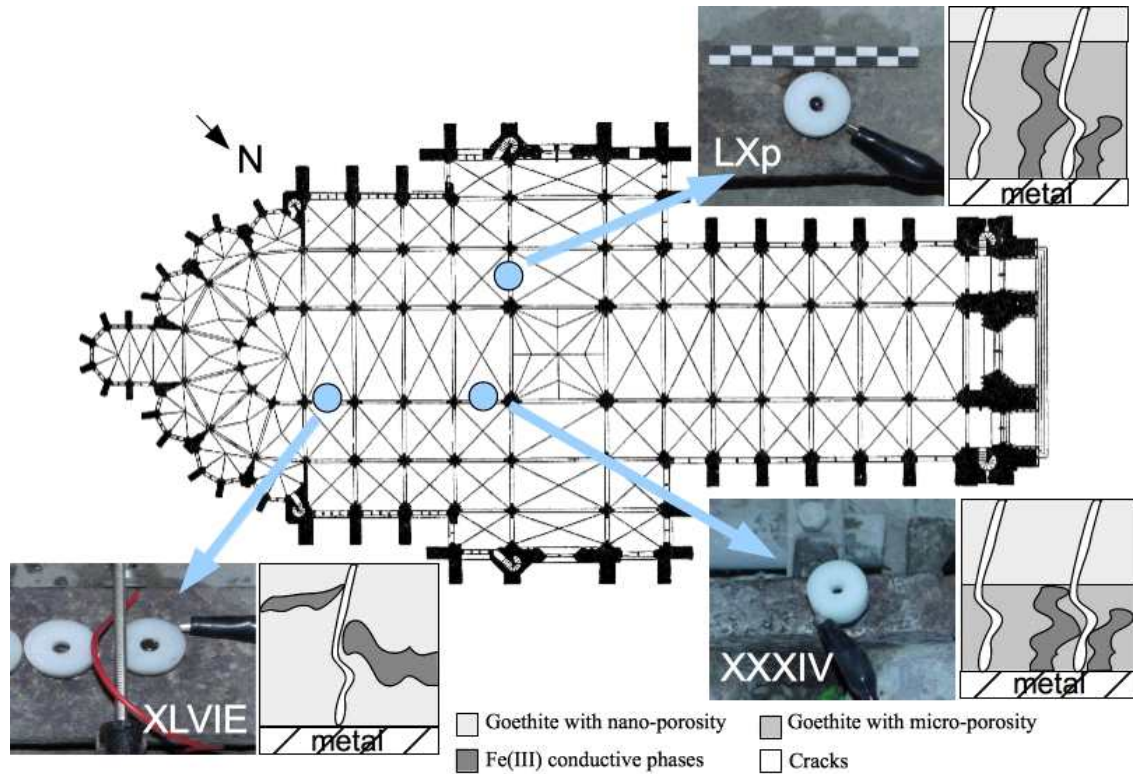


Fig. 4 Map of the Notre Dame Cathedral in Amiens with the indication of the areas submitted to the EIS measurements and a schematic representation of the cross-section of the corrosion layer.

the cross-sections of the corrosion layers allows to measure a thickness of the oxidized zone ranging from 90 to 210  $\mu\text{m}$ .

In situ EIS measurements have been employed to investigate the phenomena involved at the electrochemical interfaces among the various corrosion products and to assess and predict their corrosion behaviour, in different areas of the Cathedral, as indicated in the map of the Cathedral in Fig. 4. The corrosion layers are characterized by the presence of cracks and by a variable porosity, that can play a very important role in the corrosion mechanism. The cracks allow the penetration of the electrolyte until the metal surface where, due to the presence of active phases, the corrosion can proceed very fast.

Fig. 5 shows some impedance measurements carried out on different areas of the Cultural Heritage asset and presented as Bode plots (impedance modulus and phase). The value of the impedance modulus,  $|Z|$ , indicates the extent of the corrosion phenomenon at the interface metal/corrosion products layer. The higher the value of the electrochemical impedance, the higher the electrochemical stability of the superficial layer and its protective effectiveness against atmospheric aggressive agents. The Bode

plot of a highly protective layer is characterised by a pure capacitive behaviour with high impedance values at low frequencies. In the case of a damaged film or of an electrochemically active layer, the impedance modulus,  $|Z|$ , decreases and a plateau develops at medium frequencies in

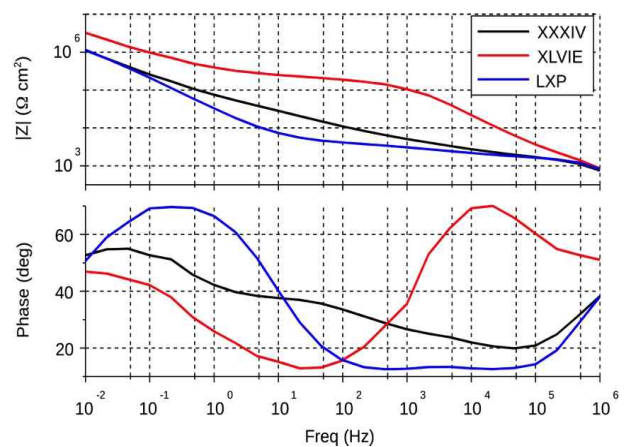
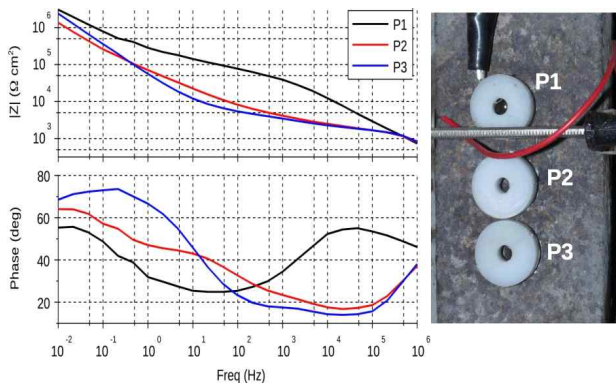


Fig. 5 EIS measurements - Bode plots recorded onto the three areas of the iron bar chain of the Notre-Dame Cathedral shown in Fig. 4.



**Fig. 6** EIS measurements - Bode plots recorded on three points of the same iron bar chain of the Notre Dame Cathedral in Amiens.

the plot.

The impedance spectra recorded on three areas of the wrought iron bar chain of the Notre Dame Cathedral in Amiens, indicated as LXp, XLVIE, XXXIV, show a different electrochemical behavior, highlighted in particular by the phase plots. All the plots show a diffusive behavior at low frequency as highlighted by the phase close to  $45^\circ$  even though with remarkable differences in the impedance amplitude. The EIS plot related to XLVIE area shows higher impedance values with respect to the plots obtained in LXp and XXXIV areas, possibly related to a lower porosity degree, and a capacitive behavior at higher frequencies, possibly related to the presence of zones where the metal is not in contact with conductive phases.

The Bode plots obtained on LXp and XXXIV areas show lower impedance values, that may be related to a higher cross porosity degree and or to the presence of cracks through the whole corrosion layer. Moreover, LXp

and XXXIV areas show a noteworthy different behaviour at intermediate frequencies: LXp shows a more capacitive behavior, that may be associated to the presence of insulating zones with limited thickness and therefore with high capacity. The Bode plot related to XXXIV area has a less pronounced capacitive behavior associated to a thick insulating layer with a lower capacity.

The corrosion products layer formed after long-lasting exposure to indoor atmosphere is highly heterogeneous. It may be described as a multiphase system, a mixture of iron oxides and oxy-hydroxides formed during the three stages (wetting, wet, and dry) of the well-known cycle [20], characterised by a variation of the thickness of the electrolyte layer in contact with the metallic surface. During the three stages, different corrosion reactions proceed leading to the formation of different phases in the rust layer.

Some phases, such as ferrihydrite ( $5\text{Fe}_2\text{O}_3 \times 9\text{H}_2\text{O}$ ), ferroxite ( $\text{d-FeOOH}$ ), poorly crystallised maghemite ( $\text{c-Fe}_2\text{O}_3$ ) and lepidocrocite ( $\text{g-FeOOH}$ ), seem to play an active role in the corrosion process; while other phases, such as goethite ( $\text{a-FeOOH}$ ), are considered stable from the electrochemical point of view.

The overall corrosion behaviour of the artefact depends on the composition of the rust layer, and on the distribution of the different phases. As a matter of facts, the most dangerous situation is related to the presence of electrochemically active Fe (III) phases directly in contact with the metal. Another important degradation factor is the presence of cracks, preferential paths for the diffusion of oxygen and other aggressive agents from the atmosphere to the metallic substrate.

The graphic inserts of Fig. 4 are a schematic representation of corrosion products layer as derived from the EIS

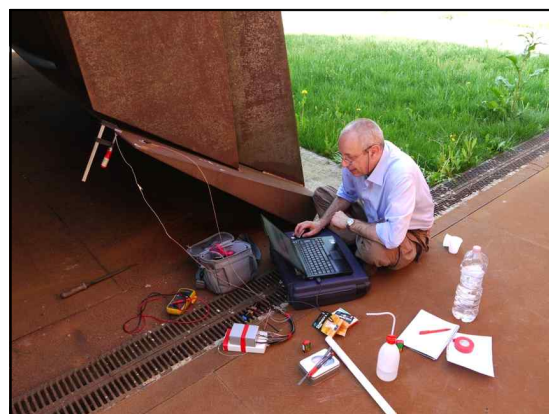


**Fig. 7** *Reditus ad origines* a sculpture in weathering steel by Agapito Miniucchi (left); in situ EIS measurements performed with the portable instrument on the sculpture (right).

measurements.

The results obtained with repeated EIS measurements carried out on the same chain in the same zone are shown in Fig. 5. The Bode plots and, in particular, the trend of the phase angle,  $f$ , evidence the presence of two time constants, although the two semicircles cannot be easily observed in the Nyquist plots, due to the large variation in the impedance amplitude.

Notwithstanding the high values of the impedance modulus,  $|Z|$ , estimated by the Bode plot at lower frequencies, in the range  $2 - 6 \text{ M}\Omega \times \text{cm}^2$ , the electrochemical behaviour of the corrosion product layer can be very different from one point to the other, even if they are very close, as highlighted by the EIS results of Fig. 6. Consequently a simple analysis of the EIS spectra taken only in one point can lead to the misleading conclusion that the corrosion product layer acts as an insulating film and protects the metallic substrate. The information is not exhaustive and representative of the real situation, therefore, a detailed investigation of the EIS results is necessary.

### 3.2 Outdoor cultural heritage asset

The second case study is a sculpture in weathering steel “Reditus ad origines”, realized in 1983 by the Italian artist Agapito Miniucchi. The sculpture, which illustrates the initiatory path of man, is exposed to the outdoor atmosphere in the Scientific and Technological Pole of Ferrara University, an interesting example of architectural recovery of an industrial area. The sculpture, shown in Fig. 7, is composed of two blocks in weathering steel, of the following dimensions:  $11 \times 5.7 \times 5.2 \text{ m}$  and  $2.5 \times 6 \times 6 \text{ m}$ . The big Cultural Heritage asset plays on the basic geometric shapes, square, rectangle, triangle, semicircle, evoking symbols of our common heritage, from the plane tuning fork to the impending beam, to the dangerous spear. The choice of the material is not unusual, as a matter of fact the main applications for weathering steels include not only civil structures such as bridges and other load-bearing structures, road installations, electricity posts, utility towers, guide rails, but also ornamental sculptures and façades and roofing. As well known, weathering steels or high-strength low alloy steels are a group of steels with the unique characteristic that as they corrode under proper conditions, they form a dense and tightly adherent oxide barrier that seals out the atmosphere and retards further corrosion [21]. The patina on weathering steel not only offers greater corrosion resistance than on mild steel, but is also responsible for its attractive appearance and self-healing abilities. The corrosion-retarding effect of the protective layer is due to the particular distribution and concentration of the alloying elements as Cu, Cr, Ni, Mn,

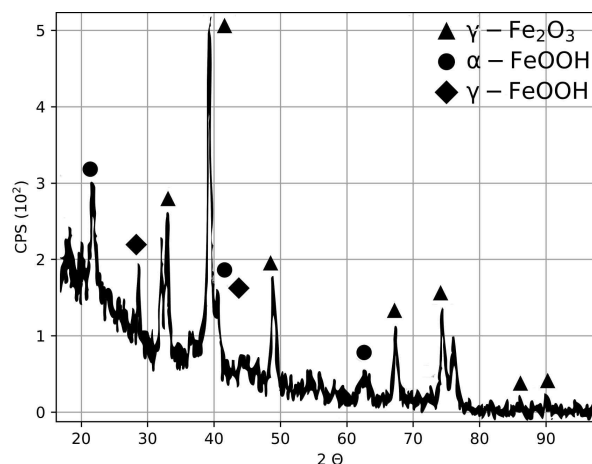


Fig. 8 - X-ray diffraction pattern of the corrosion products layers formed on the weathering steel sculpture *Reditus ad Origines*.

etc., added in amounts of 0.2 - 0.3 wt%. The rust develops and regenerates continuously when subjected to the influence of the weather. The formation of the protective layer may be adversely affected by different environmental factors, as temperature and humidity and the presence of aggressive gaseous pollutants ( $\text{SO}_2$ ,  $\text{NO}_x$ , etc) in the atmosphere.

The sculpture under study, like most outdoor weathering steel artefacts, shows areas with different colours of the rust layer depending on the orientation of the metal plates and localized corrosion attacks on some weldments. The characterization and monitoring campaign was carried out on several areas of the artefact surface, exposed to different orientations (South-West and North-East) and characterised by corrosion product layer of different colours and morphology. A noticeable part of the surface of the external walls is covered by a uniform well-adherent red-orange layer of corrosion products as the semicircular-shaped side of the sculpture, constantly exposed to sunlight. The other geometric shaped parts of the sculpture are mainly covered by a well-adherent red-brown corrosion product layer. The interstitial regions of the sculpture, the weldment areas, are subjected to some extent to localized attacks. Some large pits are observed with a consequent localized decrease of the thickness of the protective corrosion products layer.

X-Ray diffraction allowed to identify in the corrosion products the presence of oxy-hydroxides such as lepidocrocite ( $\gamma\text{-FeOOH}$ ) and goethite ( $\alpha\text{-FeOOH}$ ), together with spinel type of iron oxides such as magnetite ( $\text{Fe}_3\text{O}_4$ ) and maghemite ( $\gamma\text{-Fe}_2\text{O}_3$ ), Fig. 8.

The latter two phases present almost identical diffracto-

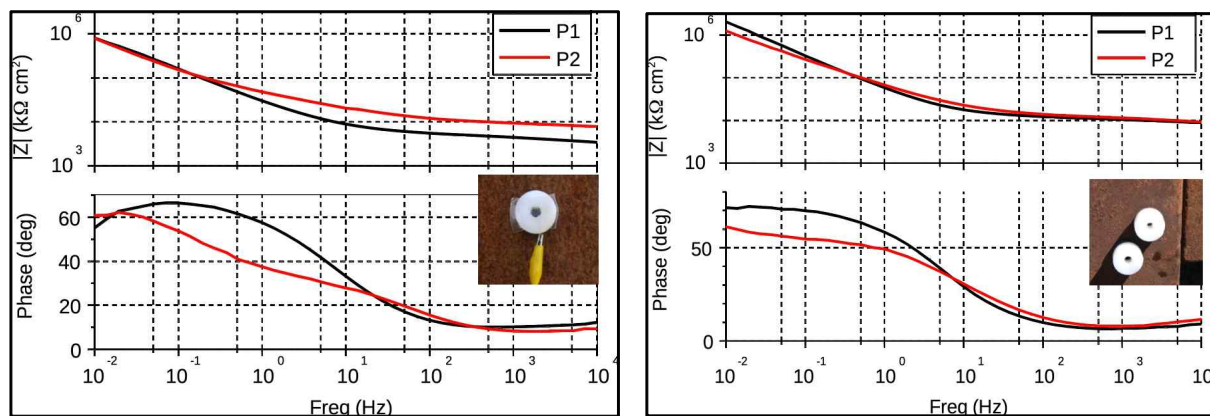


**Fig. 9. Bode plots recorded onto different areas of the sculpture *Reditus ad origines*: red-orange iron oxides (top), red-brown iron oxides (bottom). P1 refers to areas in the South -West side of the sculpture; P2 refers to areas of the North-East side of the sculpture.**

grams and their identification by XRD alone is complicated when they are mixed with large amounts of lepidocrocite and goethite [22]; furthermore the presence of amorphous phases increases the difficulty of a complete identification of the rust layer. Notwithstanding these problems, a prevalence of lepidocrocite may be observed in the red-orange area of corrosion products, while in the dark-brown area a prevalence of goethite and magnetite may be found.

In Fig. 9 the results of a monitoring campaign carried out by means of in situ EIS measurements allow to relate the different visual appearance and morphology of the corrosion products layer with their protective effectiveness. In particular the impedance spectra representative of the two surface conditions, above mentioned, the red-orange and the red-brown layer, are presented as Bode diagrams, impedance modulus and phase. The areas of the sculpture covered with the red-orange corrosion product layer show the lower impedance modulus,  $|Z|$ , values, from 3 to 8 k $\Omega$ . The phase changes vary from 40° to 0° thus indicating that the corrosion process is still in progress and involves mass transfer diffusion effects. The low  $|Z|$  values can be related to a lower thickness of the corrosion product layer, which is still growing onto the surface and has not yet reached a stable condition. Impedance values, one order of magnitude higher, are measured in the red-brown areas.  $|Z|$  values are higher than 100 k $\Omega$ , indicating that the surface is coated by a more homogeneous and well-adherent corrosion layer. The phase trends are characterized by one-time constant and involve mass transfer diffusion effects. Notwithstanding the differences in the EIS data of the various areas of the sculpture, the conservation condition of the Cultural Heritage asset can be considered acceptable.

A series of tests have been planned on the sculpture on an annual basis in order to monitor the evolution of the protective effectiveness of the iron oxides layer in the different areas.

#### 4. Conclusions

The results of the EIS measurements evidence how employing a simple test, which can be performed in situ without damaging the artefacts, it is possible to gain quickly a knowledge of the conservation state of the metallic cultural asset, highlighting potential danger conditions.

The iron bar chain of the Notre-Dame Amiens cathedral is coated by corrosion products constituted by iron oxides and oxy-hydroxides organised in a very complex structure: in this case EIS measurements allowed to investigate the electrochemical behaviour of the different compounds present in the corrosion products layers. Since  $R_{ct}$ , the charge transfer resistance, is mainly connected to the capability of the ions to penetrate the layers inducing corrosion phenomena: high values are related to the presence of stable phases, such as goethite, and low amount of ferrihydrite; low  $R_{ct}$  values are related to the presence of ferrihydrite-type

In the case of the weathering steel monument, the EIS measurements were carried out to correlate the different visual appearance and morphology with the protective effectiveness of the corrosion products layer. reactive phases.

The EIS approach integrates the morphological and structural analyses as SEM and XRD, performed to understand the chemical nature of the corrosion layers. EIS measurements gave important information on the morphology and on the adhesion of the corrosion products

layers to the metallic substrate evidencing also the presence of cracks.

Non-invasive techniques to assess the conservation state of the metallic Cultural Heritage assets are the starting point for developing tailored approaches for stopping degradation and preventing further damages.

## References

1. A. J. Howard, *Int. J. Herit. Stud.*, **19**, 632 (2013).
2. B. Marzeion and A. Levermann, *Environmental Research Letters*, **9**, Article No. 034001 (2014).
3. D. De la Fuente, J. M. Vega, F. Viejo, I. Diaz, and M. Morcillo, *J. Cult. Herit.*, **14**, 138 (2013).
4. I. Rorig-Dalgaard, *Mater. Struct.*, **46**, 959 (2013).
5. P. C. Dawson, M. M. Bertulli, R. Levy, C. Tucker, L. Dick, and P. L. Cousins, Application of 3D Laser Scanning to the Preservation of Fort Conger, a Historic Polar Research Base on Northern Ellesmere Island, Arctic Canada, *Arctic*, **66**, 147 (2013).
6. Z. Huijbregts, R. P. Kramer, M. H. J. Martens, A. W. M. van Schijndel, and H. L. Schellen, *Build. Environ.*, **55**, 43 (2012).
7. F. J. Garcia-Diego, A. Fernandez-Navajas, P. Beltran, and P. Merello, Study of the Effect of the Strategy of Heating on the Mudejar Church of Santa Maria in Ateca (Spain) for Preventive Conservation of the Altarpiece Surroundings, *Sensors*, **13**, 11407 (2013).
8. E. Angelini, S. Grassini, D. Mombello, A. Neri, and M. Parvis, *Appl. Mech. Mater.*, **100**, 919 (2010).
9. E. Angelini, T. De Caro, A. Mezzi, C. Riccucci, F. Farandi, and S. Grassini, *Surf. Interface Anal.*, **44**, 947 (2012).
10. G. M. Ingo, G. Guida, E. Angelini, G. Di Carlo, A. Mezzi, and G. Padeletti, *Accounts Chem. Res.*, **46**, 2365 (2013).
11. M. A. Emami and M. Bighan, *Surf. Eng.*, **29**, 128 (2013).
12. E. Rocca and F. Mirambet, *J. Solid State Electrochem.*, **14**, 415 (2010).
13. V. Costa and L. Robbiola, *Actual. Chimique*, **327-28**, 27-32 (2009).
14. S. Grassini, Electrochemical Impedance Spectroscopy (EIS) for the in-situ analysis of metallic heritage artefacts (In) Corrosion and conservation of cultural heritage metallic artefacts / P.Dillmann, D. Watkinson, E. Angelini, A. Adriens (EFC-WP21 on Corrosion of Archaeological and Historical Artefacts), pp. 347-367, Woodhead Publishing Limited, Cambridge (2013).
15. E. Cano, D. Lafuente, and D. M. Bastidas, *J. Solid State Electrochem.*, **14**, 381 (2010).
16. E. Angelini, S. Corbellini, M. Parvis, F. Ferraris, and S. Grassini, *Proc. Instrumentation and Measurement Technology Conf., I2MTC2014*, May 12-15, Montevideo, Uruguay (2014).
17. E. Angelini, A. Carullo, S. Corbellini, F. Ferraris, V. Gallone, S. Grassini, M. Parvis, and A. Vallan, *IEEE T. Instrum/ Meas.*, **55**, 436 (2006).
18. E. Barsoukov and J. R. Macdonald, *Impedance Spectroscopy: Theory, Experiment and Applications*, Eds., Wiley- Interscience (2005).
19. J. Monnier, L. Bellot-Gurlet, D. Baron, D. Neff, I. Guillot, and P. Dillmann, *J. Raman Spectrosc.*, **42**, 773 (2011).
20. M. Stratmann, *Proc. 201st Meeting*, Corrosion Science; A retrospective and current status in honor of Robert, 13, pp. 89 - 103, Electrochemical Society Series, Abstract No. 308, Philadelphia (2002).
21. M. Morcillo, I. Diaz, B. Chico, H. Cano, and D. de la Fuente, *Corros. Sci.*, **83**, 6 (2014).
22. P. Montoya, I. Diaz, N. Granizo, D. de la Fuente, and M. Morcillo, *Mater. Chem. Phys.*, **142**, 220 (2013).